Comparison of the Three-Dimensional Accuracy of Guided Apicoectomy Performed with a Drill or a Trephine: An In Vitro Study

Ramóna Kiscsatári [1], Eszter Nagy [2], Máté Szabó [2], Gábor Braunitzer [3], József Piffkó [1], Márk Fráter [2] and Márk Ádám Antal [2,4,*]

1 Department of Oral and Maxillofacial Surgery, Faculty of Medicine, University of Szeged, 6725 Szeged, Hungary; ramonakiscsatari@gmail.com (R.K.); piffko.jozsef@med.u-szeged.hu (J.P.)

2 Department of Operative and Esthetic Dentistry, Faculty of Dentistry, University of Szeged, 6720 Szeged, Hungary; eszthu@gmail.com (E.N.); matetaylors@gmail.com (M.S.); meddentist.fm@gmail.com (M.F.)

3 dicomLAB Dental, Ltd., 6726 Szeged, Hungary; braunitzergabor@gmail.com

4 Department of Preventive and Restorative Dentistry, College of Dental Medicine, University of Sharjah, Sharjah P.O. Box 27272, United Arab Emirates

* Correspondence: antal.mark@szte.hu; Tel.: +36-62-545-283

Abstract: Guided apicoectomy performed with 3D-printed polymer-based static surgical guides is an emerging trend in endodontic surgery. Static-guided apicoectomy is carried out with either a drill or a trephine. The aim of this in vitro study was to assess the accuracy of osteotomy and apicoectomy performed through a polymer guide, with both drill and trephine, and to compare the accuracy achievable with the two instruments. Six plaster models of a maxilla master model with extracted human maxillary teeth in polymethyl-methacrylate resin were used. The modeled osteotomies were performed in these. The master model was CBCT-scanned, and digital surgical plans were prepared, based on which the surgical guides were printed. The plans contained both drill and trephine apicoectomies. Digital three-dimensional position analysis was performed with dedicated algorithms. A total of 39 drill and 47 trephine osteotomies were analyzed. A statistically significant difference between the two instruments was found only in the global deviation of the distal endpoint, indicating lower deviation for the trephine procedure (1.53 mm vs. 1.31 mm, *p* = 0.038). Nevertheless, from a clinical perspective, this distinction is inconsequential. The results suggest that, for all practical purposes, the two approaches to apicoectomy allow the same level of accuracy.

Keywords: endodontic microsurgery; apicoectomy; 3D printing; static surgical guide

1. Introduction

Periapical surgery aims at treating persistent endodontic pathosis remaining after conventional root canal therapy [1–3]. The past 30 years have seen immense development in this field. Nowadays, periapical surgery is mostly performed as endodontic microsurgery, and it should be so, given the advantages of this approach over the conventional method [4,5]. Endodontic microsurgery amalgamates the benefits of magnification and illumination offered by the microscope, integrates modern microinstruments alongside microsurgical techniques, and employs biomaterials [4,6–8]. With these improvements, the success rate has increased from 44.2–53.5% (conventional periapical surgery) to 90.5–91.1% (endodontic microsurgery) [9,10]. Despite these technological improvements, the success of surgical treatments is highly influenced by the operator factor as well. The experience of the dentist or the surgeon is a key factor during any intervention. Several studies suggested that guided surgeries may be of superior precision compared with freehand manipulation. Pinsky and colleagues indicated that surgical guidance can offer enhanced precision and consistency in endodontic surgery, with added benefits of three-dimensional presurgical

visualization [11]. Giacomino and colleagues highlighted the effectiveness of trephine burs when guided by 3D surgical guides, demonstrating their ability to achieve precise osteotomies, with predictable positioning, angulation, and depth of preparation [12]. The findings of Hawkins et al., drawn from simulated surgery on 3D-printed teeth, support the notion that guided endodontic microsurgery yields improved osteotomy and resection outcomes, along with optimal root-end resection volume and bevel angle [13]. Additionally, Buniag et al., through a retrospective analysis of 24 cases, concluded that guided trephine bur root-end resection yields comparable success rates to the established outcomes of freehand bur resection [14]. Irrespective of performing traditional periapical surgery or modern endodontic microsurgery, it is essential to surgically remove the apical 3 mm of the root along with the persistent periapical lesion [5,15]. This requires a skilled operator, visualization, and accuracy. Digitalization, in the form of routinely using CBCT in endodontic microsurgery cases, facilitates accurate diagnosis and meticulous case evaluation. It enables precise localization of the root apex and the adjacent periapical lesion, while also safeguarding delicate neighboring tissues [16,17]. A CBCT image with appropriate resolution can also help us decide in which cases a periapical surgical procedure can be safely performed and in which cases it should be avoided owing to the close proximity of vital anatomical structures [18]. Still, adequate root resection without unnecessary tissue removal remains a challenge [19]. Endodontic microsurgery can be further simplified by using digitally planned, 3D-printed, polymer-based templates and guides for certain steps during the procedure [20]. Digital guides have been used for endodontic microsurgery since 2007 [21]. Pinsky and colleagues virtually planned osteotomies with the help of an implant planning software (CADImplant Inc., Burlington, MA, USA), and five examiners performed freehand and guided apicoectomy via the CAD/CAM templates according to the 3D plan [11]. However, the method was inchoate: it laid the foundation for guided endodontic surgical interventions, demonstrating its higher accuracy. Since then, polymer-based templates and guides have been used for multiple purposes, gradually improving and adding more features to achieve the required accuracy and to aid root-end resection at any given point of the oral cavity [12,22,23]. The first step was to accurately define the osteotomy window [24], and even to retract soft tissues during endodontic surgery [25]. These actions were only intended to make the surgical intervention manageable and easier, without any guidance at the apicoectomy itself. The most modern way to perform endodontic microsurgery is through targeted endodontic microsurgery (TEMS), which utilizes digitally designed, 3D-printed surgical guides to aid endodontic microsurgery [26]. It replaces the conventional diamond or carbide bur with an end-cutting trephine bur via a guided approach. When a trephine bur is used, the osteotomy and the removal of the apex can be carried out in one step [12]. The guidance makes this procedure less invasive, more accurate, and faster. Certain studies showed that the surgical time can be reduced to 1/3 of its original time, while the volume of removed root and over-resection is significantly less than in endodontic microsurgery (EMS) [13,14]. Regarding the bevel angles, the digitally planned and template-navigated cutting line seems to open significantly less dentinal tubules, which has a direct effect on the success and survival of these teeth [27]. Furthermore, due to the one-step approach, the less-time-consuming procedure can reduce the mental stress of the patient. [28]. This, in turn, may result in better healing outcomes, which have long been desired by both surgeons and patients [29]. However, few published data are available on whether using a normal straight (pilot) drill or a trephine bur for TEMS makes a significant difference in terms of accuracy [13,30,31]. Our goal with this preclinical study was to examine this question.

2. Materials and Methods

2.1. Model Preparation and Imaging

A maxilla master model was prepared from extracted human maxillary teeth (Figure 1). Teeth with fully developed apices were selected for this study and were not extracted for the sake of the experiment. Teeth with coronal restoration were not excluded. All teeth

were embedded in polymethyl-methacrylate resin, in their appropriate anatomical position (Figure 2A). A CBCT image was captured using an i-CAT Next Generation device (Imaging Sciences—Kavo, Hatfield, PA, USA) employing the subsequent parameters: tube voltage: 120 kV; tube current: 5 mA; exposure time: 14.7 s; voxel size: 250 μm; and field of view (FOV): 160 × 130 mm. The model was then scanned using an extraoral desktop scanner (Maestro 3D MDS400, AGE Solutions, Pontedera, Italy) at 70 μm resolution. The DICOM and the STL data were superimposed in digital planning software for guided dental surgery (Smart Guide Software System, dicomLAB Dental Ltd., Szeged, Hungary).
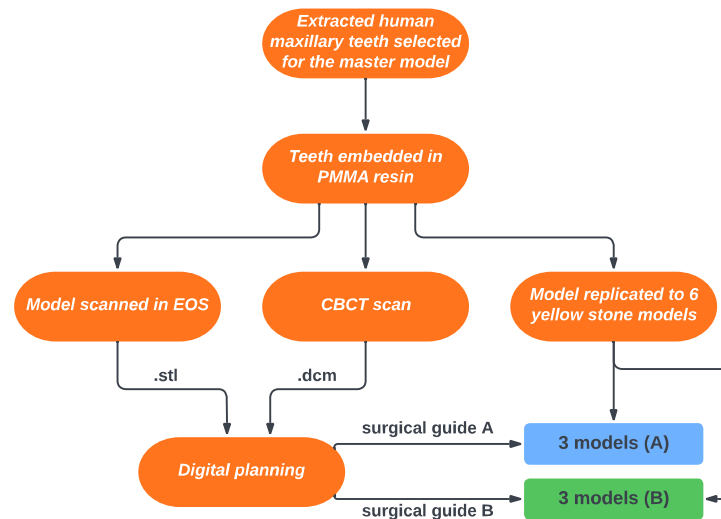
Figure 1. Flow diagram of model and surgical guide preparation.
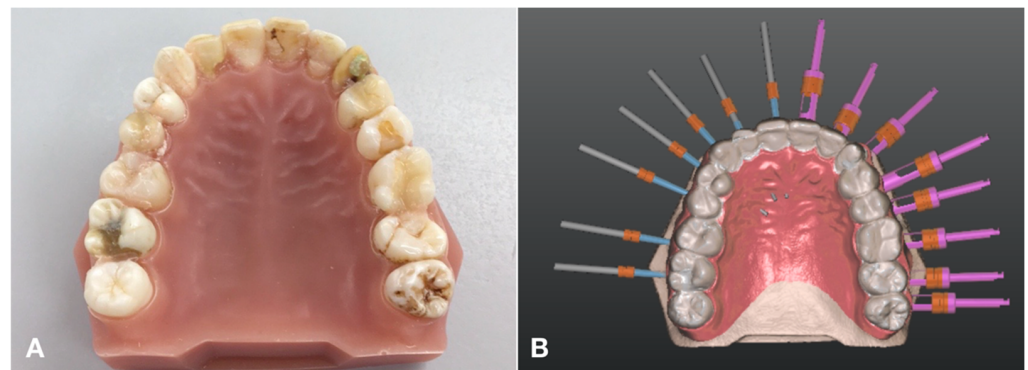
Figure 2. (**A**) Human teeth embedded in polymethyl-methacrylate resin. (**B**) The virtual 3D plan of Setup A (plan A) with trephines on the right side and pilot drills on the left side.

2.2. Planning

Two 3D surgical plans were prepared by an operator with over a decade of experience in static-guided dental surgical planning. In plan A, drills were planned on the left side and trephine burs on the right side (Figure 2B). In plan B, the sides were swapped. The instruments always targeted the apices of the roots of the corresponding teeth. The drill procedures were planned in the pilot drill setting of the planning software module using cylindrical implant models 2 mm in diameter to simulate the drill. The trephine procedures were planned with the digital model of the instrument itself (Figure 3). Both models were of the same length, helping the operator to plan the surgery the same way on both sides (Figure 4).
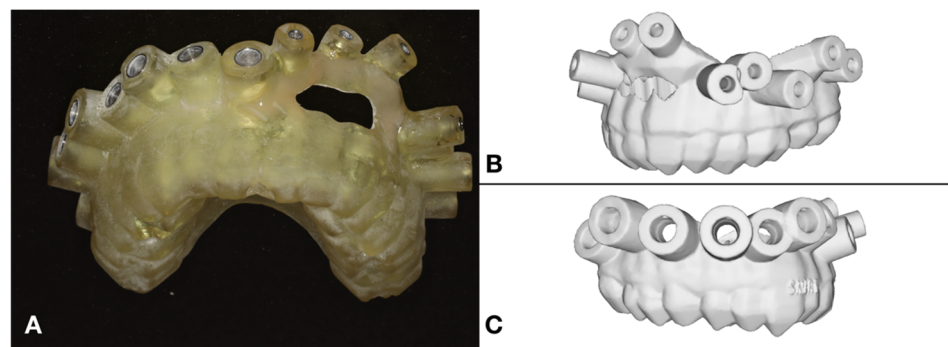
Figure 3. (**A**) The 3D-printed polymer surgical guide with the metal guiding sleeves. (**B**) The virtual plan of the guide as viewed from the left side. (**C**) The virtual plan of the guide as viewed from the right side.
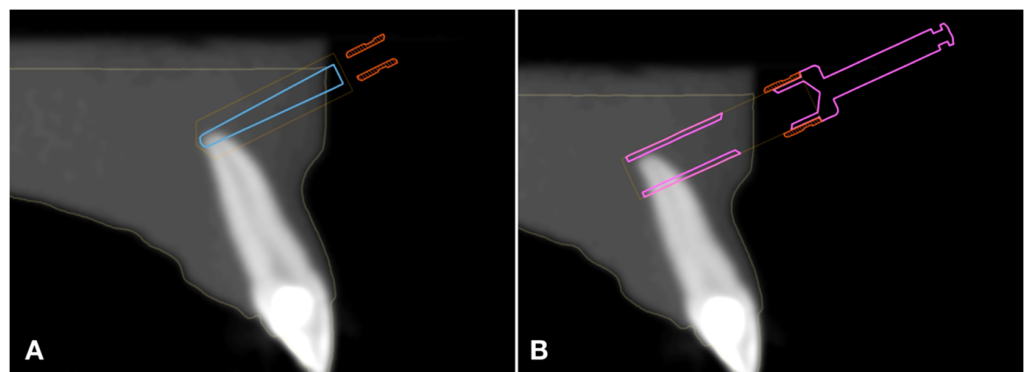
Figure 4. (**A**) Digital surgical plan (orovestibular view) for tooth 22 (orovestibular view, plan A, pilot drill). (**B**) Digital surgical plan for tooth 22 (orovestibular view, plan B, trephine). Note that for the planning of the drill procedures, the virtual model of an implant 2 mm in diameter was used, as a model of a drill was not available in the software.

2.3. The Surgical Guide and the Applied Instruments

The surgical guides were 3D-printed with a ProJet MD3510 multijet printer (3D Systems, Rock Hill, SC, USA). The actual instruments were used through metal sleeves embedded in the 3D-printed polymer body of the surgical guide. In the case of the pilot drills, exactly matching metal sleeves were placed with an inner diameter of 2.04 mm for the 2.00 mm diameter stainless steel pilot drills. As for the trephines, 4.46 mm endo-trephines were used through a 4.50 mm guiding sleeve, as described in our earlier studies [23,30]. The instruments are shown in Figure 5.

Figure 5. (**A**) Pilot drill with a diameter of 2 mm and a depth stop at a 20 mm length. (**B**) Endo-trephine with a diameter of 4.46 mm with a depth stop at a 20 mm length.

2.4. Simulated Surgery and Postoperative Analysis

The master model was replicated in polyvinyl siloxane (Ecosil, Dentarum, Ispringen, Germany) in 6 yellow plaster models (Hiro HardRock, Mutsumi Chemical Industries Co., Ltd., Yokkaichi, Japan). Of the six models, three were used in group A (plan A) and three in group B (plan B). Once the simulated osteotomies had been performed, CBCT images were taken of the plaster models with the same settings as described above. Preoperative and postoperative DICOM data were superimposed and compared in Amira 5.4.5 (Thermo Fisher Scientific, Waltham, MA, USA). In the postoperative scans, metal cylinders were carefully introduced into the cylindrical cavities created by the osteotomies, with dimensions matching the length and diameter of the utilized drills and trephines. This step was imperative due to the segmentation-based nature of the analysis, which relies on grayscale values to distinguish between distinct objects. It is worth noting that this methodology was previously examined and documented [30]. The measurements involved a registration process where the preoperative and postoperative CBCT scans were aligned within a consistent coordinate system. Subsequently, the metal cylinders employed for the postoperative scans (as previously described) underwent segmentation and were then digitally transformed into virtual bodies. Virtual cylinders representing and corresponding to either of the two instruments were aligned with these segmented bodies along their principal axes. The spatial position of such a cylinder (after alignment) represented the achieved position of the instrument in the model. Subsequently, the process encompassed the reconstruction of the anticipated positions. Virtual cylinders were employed for this purpose, with their dimensions mirroring those of the respective instrument. The intended instrument position was derived from the digital surgical plan and then superimposed onto the cylinder. The outcome of this procedure yielded two virtual cylinders that partially overlapped: one denoting the projected instrument position and the other representing the attained position.

Consequently, this approach enabled a direct comparison between the osteotomy outcome and the plan (Figure 6). Two key variables were taken into account: distal global deviation (DGD), which signifies the distance between the distal endpoints of the virtual cylinders in millimeters; and angular deviation (AD), quantified as the angle formed by the principal axes of the aligned virtual cylinders, expressed in degrees.

The process was replicated three times for each case, and the average of the three measurements was employed for subsequent analyses [31].

2.5. Statistical Analyses

The statistical analyses were performed in SPSS 23.0 (IBM, Armonk, NY, USA). In addition to calculating the descriptive statistics (means, standard deviations, medians, and 95% confidence intervals), multiple linear regression analyses and ANOVA were performed. In the multiple linear regression model, the following variables were defined as the predictor variables: plan version (A or B), position within the dental arch (according to the FDI system), instrument (drill or trephine), and the number of the specific plaster model in which the simulated surgeries were performed (1 to 6). DGD and AD were the dependent variables.
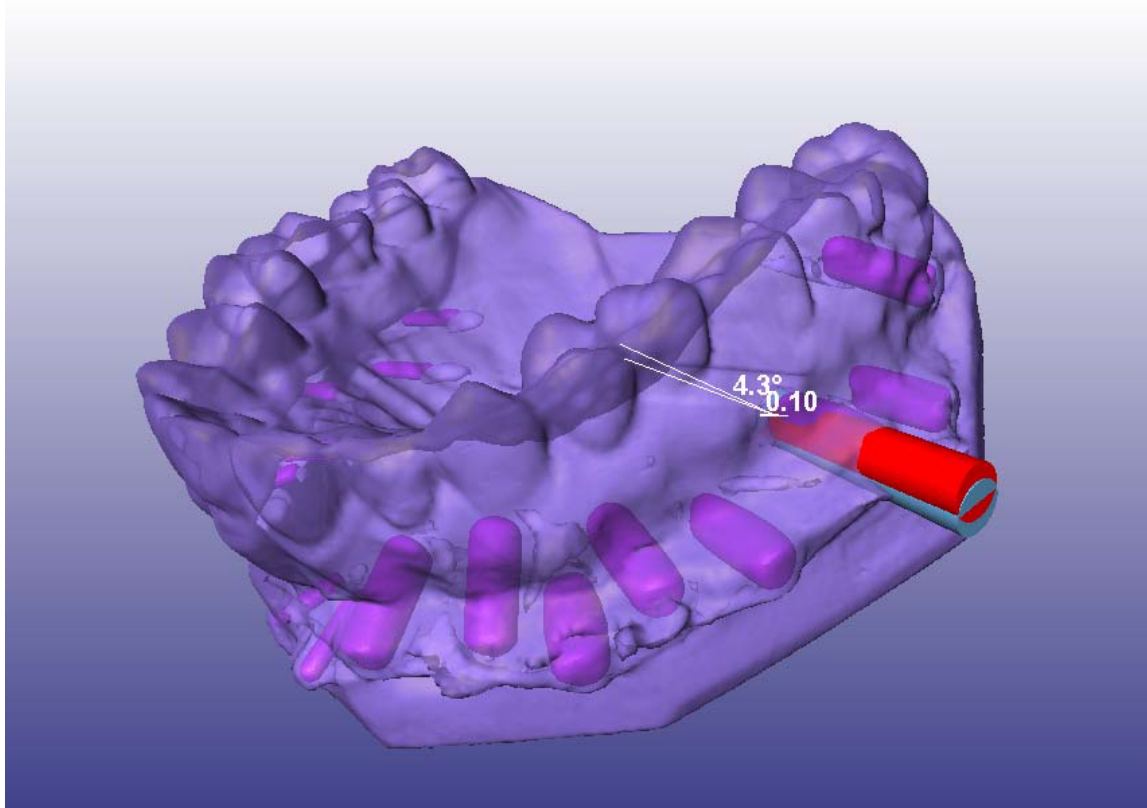
Figure 6. Analysis of a trephine procedure. The numbers show the values of distal global deviation (0.1 mm) and angular deviation (4.3°) for the given pair of virtual cylinders that represent the planned (blue) and achieved (red) instrument positions. The purple cylindrical bodies within the virtual rendering of the plaster model show the positions of the postoperatively inserted metal cylinders used as segmentation aids (see text).

3. Results

In total, 90 procedures were planned. The data of four procedures were excluded from the analysis due to alignment error. Therefore, the data of 86 procedures were analyzed. Of these, 39 (45.34%) were performed with a drill and 47 (54.65%) with a trephine. Descriptive statistics can be seen in Table 1. In the case of the drill, the DGD was 1.53 ± 0.51 mm, and the AD was $3.32 \pm 1.41°$. In contrast, in the case of the trephine, the DGD was 1.31 ± 0.45 mm, and the AD was $3.5 \pm 1.67°$.

Table 1. Descriptive statistics of the results. DGD (distal global deviation—mm), AD (angular deviation—degree).

		Drill	**Trephine**
DGD	Mean	1.5318	1.3119
	SD	0.51074	0.45690
	Median	1.4500	1.3300
	Minimum	0.60	0.46
	Maximum	3.45	2.58
AD	Mean	3.323	3.500
	SD	1.4199	1.6722
	Median	3.200	3.200
	Minimum	0.9	0.6
	Maximum	6.5	8.8

3.1. Distal Global Deviation

The multiple linear regression analysis indicated a moderately significant effect of the applied instrument ($\beta = -0.23$, $p = 0.036$). The rest of the predictors did not have a significant effect on this parameter.

The mean DGD was 1.531 ± 0.510 mm (median: 1.45 mm, 95% CI: 1.366–1.697) for the pilot drills and 1.311 ± 0.456 mm (median: 1.33 mm, 95% CI: 1.177–1.446) for the trephines (Figure 7). The difference was moderately significant, as indicated by ANOVA (F = 4.44, df = 1, $p = 0.038$). The effect size was small (f = 0.19).
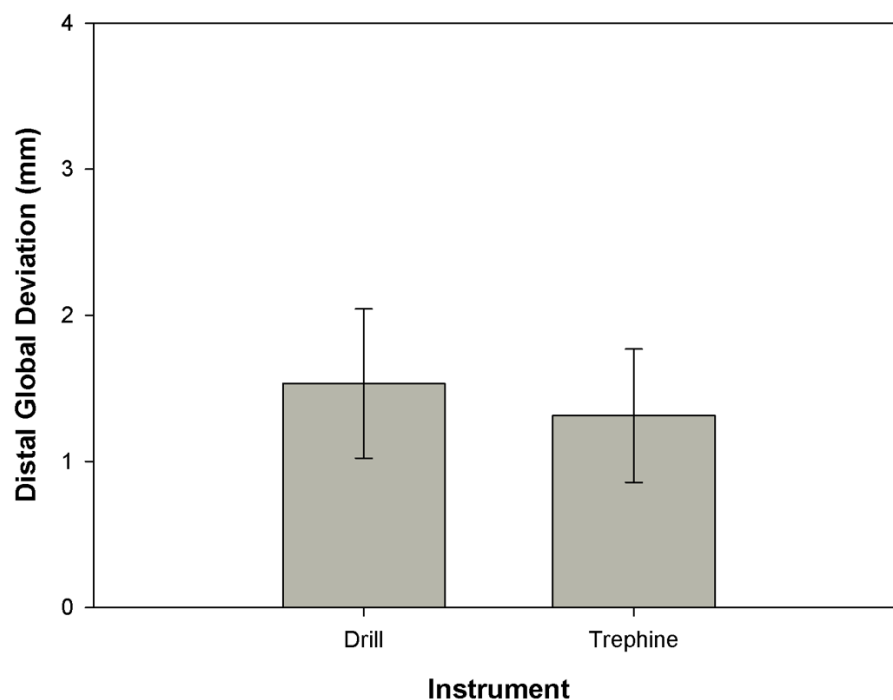
Figure 7. A comparison of distal global deviation (DGD) between the drill and the trephine procedures (mean $\pm$ SD).

3.2. Angular Deviation

The multiple linear regression analysis did not indicate a significant effect for any of the predictors. The mean AD was $3.323 \pm 1.419°$ (median: 3.2°, 95% CI: 2.863–3.783) for the pilot drills and $3.500 \pm 1.672°$ (median: 3.2°, 95% CI: 3.009–3.991) for the trephines.

4. Discussion

In recent years, several case reports [12,22,32–34] and case series [14,31] have dealt with TEMS as an emerging method of endodontic microsurgery, performed with either a pilot drill or a trephine. In the investigation conducted by Ye et al., a digitally designed directional template proved to be a comprehensive facilitator for periapical surgery, surpassing initial expectations. The precision of root-end localization and resection was consistently achieved, simplifying the surgical procedure and elevating treatment efficiency. Notably, this technique demonstrated significant reductions in both damage and iatrogenic injury [22]. Strbac et al. identified the guided microsurgical endodontic approach as a practicable method enabling predefined osteotomies and root resections [32]. Ahn et al. likewise established the utility of a CAD/CAM-guided surgical template in addressing intricate endodontic surgery scenarios [34]. Demonstrating the efficacy of a trephine-bur-assisted approach, Nagy et al. highlighted the superior speed and precision achieved compared with nonguided endodontic microsurgery [33]. Buniag et al.'s investigation endorsed TEMS-guided trephine bur root-end resection as comparably successful to conventional freehand bur resection [14]. Conclusively, Antal et al.'s case series' findings endorsed the viability of guided trephination for root-end resection [31]. While the pilot drill approach

necessitates the subsequent extension of the osteotomy and the resection of the root end as a separate step, TEMS performed with a trephine is usually reported to make additional steps unnecessary. However, very few data are available about the accuracy of these techniques. The first preclinical study of this kind was published in 2007. In this 2007 study, Pinsky and colleagues compared the use of a guided pilot drill with freehand osteotomy [11]. In their research, the DGD was found to be 0.79 ± 0.33 mm for the procedures performed with guided pilot drills and 2.27 ± 1.46 mm for the freehand procedures. It appears that the authors found a higher accuracy for the pilot drill procedure than we have in the present study (1.531 ± 0.510 mm). The results are hard to compare; however, the pilot drill deviations in both studies are significantly smaller than those of the freehand results. On the one hand, the comparison is difficult because the Pinsky group superimposed the pre- and postoperative models manually. Today, this is performed automatically based on grayscale values [30,35], which makes the analysis more objective and reliable. In this study, we used grayscale-based digital superimposition too. On the other hand, Pinsky et al. did not give an in-depth description of their study sample. It was mentioned that five operators performed osteotomies in all teeth in a duplicated mandible model, but exact numbers (e.g., about the number of the performed procedures) are not given at all: it only provides the 'operator factor', as aforementioned, to rule out this important feature during EMS procedures. Nevertheless, the study of the Pinsky group can still be regarded as pioneering, with an essentially sound methodology. It was for this reason that we decided to take the same approach enhanced with up-to-date digital methods.

Comparing the accuracy of the procedures performed with a pilot drill and a trephine, we found that the trephine procedure was characterized by a significantly smaller DGD (higher accuracy). However, it must be noted that the difference was quite small (0.22 mm between the means and 0.12 mm between the medians). From a clinical point of view, such a small difference is probably negligible. The correct interpretation of the results is probably that trephine TEMS is comparable to pilot drill TEMS in terms of accuracy (the latter being significantly more accurate than the conventional freehand approach, as shown in previous studies [29,31]). As the accuracy of all surgical procedures is multifactorial, every single parameter can gain overall success. Fortunately, the depth of apicoectomy is less than other guided surgical interventions'; in this way, the difference in DGD can be decreased while maintaining the same importance in practice.

Our research group already published accurate data about trephine osteotomy [26]. That study concentrated on the contribution of the depth stop to the accuracy of the procedure. The mean DGD was 0.92 mm when the trephine had a depth stop and 2.35 mm when it did not. Naturally, only the data from the depth stop trephine group can be compared with the data of the present study. One should not overlook the fact, however, that our previous study was carried out in porcine mandibles to provide human-like circumstances during apicoectomy. The mineral content and bone hardness of the porcine mandible are similar to those of human bones, which suggests that the trephine can be more precise in realistic conditions when the penetration depth is under physical control [36–39].

Another preclinical study was published by Gaffuri et al. in 2021 [40]. The authors performed 40 osteotomies on cadavers. Trephine osteotomies were performed without a control group. The mean DGD was 1.23 ± 0.38 mm, which is almost the same as what we found in this study. They further emphasized that there was no noteworthy distinction in the precision of osteotomies performed by experienced surgeons and dental students, thereby demonstrating the applicability of this approach to ensure the safety of apicoectomy across varying levels of expertise.

As for AD, this is a parameter that is usually not reported in the literature in connection with TEMS (in contrast to studies on the accuracy dental implantology), while angulation is obviously not irrelevant in this context either. AD can have a severe effect on the precision during the removal of the apical 3 mm, since the presence of lateral canals and ramification in the apical third are the common causes of persisting apical infection [41]. Any deviation in this area can result in the failure to remove the infected tissue, hindering the healing

chances and the survival of the tooth. In this respect, our study definitely offers new information. In this study, we found a mean AD of 3.3° for the pilot drills and 3.5° for the trephines. As said, due to the lack of data, a direct comparison with other TEMS studies is not possible, but in the literature on guided dental implantology, similar values are associated with the highest achievable accuracy [35,42–45]. As the method itself is based on the guided implantation steps, the results found by Younes et al. on freehand-guided pilot and fully guided drilling can help to compare our results. The fully guided procedure was significantly better (2.30°, standard error 0.92°) regarding AD than the accuracy of the freehand (6.99°, standard error 0.87°) or guided pilot (5.95°, standard error 0.87°) group [42]. The main reason why implant guide studies can provide slightly better AD results is probably the difference in the support of the guide. In most surgical studies, the guide is tooth-supported, while in the case of periapical surgery, the guide extends into the vestibulum, modifying the support from dental to muco-dental or dento-mucosal. This seemingly small alteration can have a severe effect on the precision of these procedures.

5. Limitations

Regarding the study's limitations, it is evident that conducting simulated surgery on a plaster model significantly diverges from live surgical scenarios. While it allows for meticulous control of potential confounding variables, it inherently provides an idealized portrayal of reality. Consequently, the generalizability of findings from a model-based study remains circumscribed. Furthermore, such studies can introduce their own confounding factors. In the present investigation, we observed that performing drilling on stone material posed distinct challenges due to its inherent hardness. The potential influence of this factor on the outcomes cannot be dismissed. In fact, considering the sturdiness and resilience of the stone, we posit that analogous procedures could yield notably improved outcomes in actual tissue environments. It is imperative to interpret the results within the context of these inherent limitations.

6. Conclusions

Taking into account the limitations of this study, our findings indicate that TEMS, irrespective of the instrument utilized, affords a level of accuracy deemed clinically acceptable. Nevertheless, validation through additional, and potentially clinical, investigations is warranted.

Author Contributions: R.K.: investigation, conceptualization, methodology, writing—original draft, visualization. E.N.: investigation, writing—review and editing. M.S.: investigation, writing—review and editing. G.B.: methodology, data curation, formal analysis, writing—review and editing. J.P.: investigation, writing—review and editing. M.F.: investigation, writing—review and editing. M.Á.A.: conceptualization, supervision, writing—original draft. All authors have read and agreed to the published version of the manuscript.

Funding: This research received no external funding.

Institutional Review Board Statement: The study adhered to the ethical guidelines outlined in the Declaration of Helsinki "Ethical Principles for Medical Research Involving Human Subjects", as ratified by the 18th World Medical Assembly in Helsinki, Finland, in June 1964, and subsequently revised by the 64th World Medical Assembly in Fortaleza, Brazil, in October 2013. The research protocol received approval from the Regional and Institutional Committee of Science and Research Ethics, University of Szeged, Hungary (Approval No.: RKEB 52/2018-SZTE).

Informed Consent Statement: Informed consent was obtained from all subjects involved in the study.

Data Availability Statement: The analysis dataset is available from the corresponding author on reasonable request.

Conflicts of Interest: The authors declare no conflict of interest.

References

1. Karabucak, B.; Setzer, F. Criteria for the ideal treatment option for failed endodontics: Surgical or nonsurgical? *Compend. Contin. Educ. Dent.* **2007**, *28*, 391–397, quiz 398, 407.
2. Tavares, W.L.F.; Fonseca, F.O.; Maia, L.M.; de Carvalho Machado, V.; Franca Alves Silva, N.R.; Junior, G.M.; Ribeiro Sobrinho, A.P. 3D Apicoectomy Guidance: Optimizing Access for Apicoectomies. *J. Oral Maxillofac. Surg.* **2020**, *78*, 357.e1. [CrossRef] [PubMed]
3. von Arx, T. Apical surgery: A review of current techniques and outcome. *Saudi Dent. J.* **2011**, *23*, 9–15. [CrossRef]
4. Kim, S.; Kratchman, S. Modern endodontic surgery concepts and practice: A review. *J. Endod.* **2006**, *32*, 601–623. [CrossRef] [PubMed]
5. Niemczyk, S.P. Essentials of endodontic microsurgery. *Dent. Clin. N. Am.* **2010**, *54*, 375–399. [CrossRef]
6. Setzer, F.C.; Kohli, M.R.; Shah, S.B.; Karabucak, B.; Kim, S. Outcome of endodontic surgery: A meta-analysis of the literature—Part 2: Comparison of endodontic microsurgical techniques with and without the use of higher magnification. *J. Endod.* **2012**, *38*, 1–10. [CrossRef] [PubMed]
7. Kohli, M.R.; Berenji, H.; Setzer, F.C.; Lee, S.M.; Karabucak, B. Outcome of Endodontic Surgery: A Meta-analysis of the Literature—Part 3: Comparison of Endodontic Microsurgical Techniques with 2 Different Root-end Filling Materials. *J. Endod.* **2018**, *44*, 923–931. [CrossRef] [PubMed]
8. Torabinejad, M.; Parirokh, M.; Dummer, P.M.H. Mineral trioxide aggregate and other bioactive endodontic cements: An updated overview—Part II: Other clinical applications and complications. *Int. Endod. J.* **2018**, *51*, 284–317. [CrossRef] [PubMed]
9. Tsesis, I.; Rosen, E.; Taschieri, S.; Telishevsky Strauss, Y.; Ceresoli, V.; Del Fabbro, M. Outcomes of surgical endodontic treatment performed by a modern technique: An updated meta-analysis of the literature. *J. Endod.* **2013**, *39*, 332–339. [CrossRef]
10. Wang, Z.H.; Zhang, M.M.; Wang, J.; Jiang, L.; Liang, Y.H. Outcomes of Endodontic Microsurgery Using a Microscope and Mineral Trioxide Aggregate: A Prospective Cohort Study. *J. Endod.* **2017**, *43*, 694–698. [CrossRef]
11. Pinsky, H.M.; Champleboux, G.; Sarment, D.P. Periapical surgery using CAD/CAM guidance: Preclinical results. *J. Endod.* **2007**, *33*, 148–151. [CrossRef] [PubMed]
12. Giacomino, C.M.; Ray, J.J.; Wealleans, J.A. Targeted Endodontic Microsurgery: A Novel Approach to Anatomically Challenging Scenarios Using 3-dimensional-printed Guides and Trephine Burs—A Report of 3 Cases. *J. Endod.* **2018**, *44*, 671–677. [CrossRef] [PubMed]
13. Hawkins, T.K.; Wealleans, J.A.; Pratt, A.M.; Ray, J.J. Targeted endodontic microsurgery and endodontic microsurgery: A surgical simulation comparison. *Int. Endod. J.* **2020**, *53*, 715–722. [CrossRef]
14. Buniag, A.G.; Pratt, A.M.; Ray, J.J. Targeted Endodontic Microsurgery: A Retrospective Outcomes Assessment of 24 Cases. *J. Endod.* **2021**, *47*, 762–769. [CrossRef]
15. Lin, S.; Platner, O.; Metzger, Z.; Tsesis, I. Residual bacteria in root apices removed by a diagonal root-end resection: A histopathological evaluation. *Int. Endod. J.* **2008**, *41*, 469–475. [CrossRef]
16. Benjamin, G.; Ather, A.; Bueno, M.R.; Estrela, C.; Diogenes, A. Preserving the Neurovascular Bundle in Targeted Endodontic Microsurgery: A Case Series. *J. Endod.* **2021**, *47*, 509–519. [CrossRef] [PubMed]
17. Patel, S.; Brown, J.; Pimentel, T.; Kelly, R.D.; Abella, F.; Durack, C. Cone beam computed tomography in Endodontics—A review of the literature. *Int. Endod. J.* **2019**, *52*, 1138–1152. [CrossRef]
18. Reda, R.; Zanza, A.; Bhandi, S.; Biase, A.; Testarelli, L.; Miccoli, G. Surgical-anatomical evaluation of mandibular premolars by CBCT among the Italian population. *Dent. Med. Probl.* **2022**, *59*, 209–216. [CrossRef]
19. Corbella, S.; Walter, C.; Tsesis, I. Effectiveness of root resection techniques compared with root canal retreatment or apical surgery for the treatment of apical periodontitis and tooth survival: A systematic review. *Int. Endod. J.* **2022**; *online ahead of print*. [CrossRef]
20. Kim, J.E.; Shim, J.S.; Shin, Y. A new minimally invasive guided endodontic microsurgery by cone beam computed tomography and 3-dimensional printing technology. *Restor. Dent. Endod.* **2019**, *44*, e29. [CrossRef]
21. Anderson, J.; Wealleans, J.; Ray, J. Endodontic applications of 3D printing. *Int. Endod. J.* **2018**, *51*, 1005–1018. [CrossRef] [PubMed]
22. Ye, S.; Zhao, S.; Wang, W.; Jiang, Q.; Yang, X. A novel method for periapical microsurgery with the aid of 3D technology: A case report. *BMC Oral Health* **2018**, *18*, 85. [CrossRef] [PubMed]
23. Antal, M.; Nagy, E.; Sanyo, L.; Braunitzer, G. Digitally Planned Root End Surgery with Static Guide and Custom Trephine Burs: A Case Report. *Int. J. Med. Robot. Comput. Assist. Surg. MRCAS* **2020**, *16*, e2115. [CrossRef] [PubMed]
24. Popowicz, W.; Palatynska-Ulatowska, A.; Kohli, M.R. Targeted Endodontic Microsurgery: Computed Tomography-based Guided Stent Approach with Platelet-rich Fibrin Graft: A Report of 2 Cases. *J. Endod.* **2019**, *45*, 1535–1542. [CrossRef]
25. Patel, S.; Aldowaisan, A.; Dawood, A. A novel method for soft tissue retraction during periapical surgery using 3D technology: A case report. *Int. Endod. J.* **2017**, *50*, 813–822. [CrossRef] [PubMed]
26. Ray, J.J.; Giacomino, C.M.; Wealleans, J.A.; Sheridan, R.R. Targeted Endodontic Microsurgery: Digital Workflow Options. *J. Endod.* **2020**, *46*, 863–871. [CrossRef]
27. Gilheany, P.A.; Figdor, D.; Tyas, M.J. Apical dentin permeability and microleakage associated with root end resection and retrograde filling. *J. Endod.* **1994**, *20*, 22–26. [CrossRef]
28. Le, S.H.; Tonami, K.; Umemori, S.; Nguyen, L.B.; Ngo, L.Q.; Araki, K.; Nitta, H. Relationship between preoperative dental anxiety and short-term inflammatory response following oral surgery. *Aust. Dent. J.* **2021**, *66*, 13–19. [CrossRef]
29. von Arx, T.; Peñarrocha, M.; Jensen, S. Prognostic factors in apical surgery with root-end filling: A meta-analysis. *J. Endod.* **2010**, *36*, 957–973. [CrossRef]

30. Nagy, E.; Braunitzer, G.; Gryschka, D.G.; Barrak, I.; Antal, M.A. Accuracy of digitally planned, guided apicoectomy with a conventional trephine and a custom-made endodontic trephine: An in vitro comparative study. *J. Stomatol. Oral Maxillofac. Surg.* **2021**, *123*, 388–394. [CrossRef]

31. Antal, M.; Nagy, E.; Braunitzer, G.; Fráter, M.; Piffkó, J. Accuracy and clinical safety of guided root end resection with a trephine: A case series. *Head Face Med.* **2019**, *15*, 30. [CrossRef] [PubMed]

32. Strbac, G.D.; Schnappauf, A.; Giannis, K.; Moritz, A.; Ulm, C. Guided Modern Endodontic Surgery: A Novel Approach for Guided Osteotomy and Root Resection. *J. Endod.* **2017**, *43*, 496–501. [CrossRef] [PubMed]

33. Nagy, E.; Fráter, M.; Antal, M. Guided modern endodontic microsurgery by use of a trephine bur. *Orv. Hetil.* **2020**, *161*, 1260–1265. [CrossRef] [PubMed]

34. Ahn, S.Y.; Kim, N.H.; Kim, S.; Karabucak, B.; Kim, E. Computer-aided Design/Computer-aided Manufacturing-guided Endodontic Surgery: Guided Osteotomy and Apex Localization in a Mandibular Molar with a Thick Buccal Bone Plate. *J. Endod.* **2018**, *44*, 665–670. [CrossRef]

35. Varga, E., Jr.; Antal, M.; Major, L.; Kiscsatári, R.; Braunitzer, G.; Piffkó, J. Guidance means accuracy: A randomized clinical trial on freehand versus guided dental implantation. *Clin. Oral Implants Res.* **2020**, *31*, 417–430. [CrossRef] [PubMed]

36. Möhlhenrich, S.C.; Modabber, A.; Steiner, T.; Mitchell, D.A.; Hölzle, F. Heat generation and drill wear during dental implant site preparation: Systematic review. *Br. J. Oral Maxillofac. Surg.* **2015**, *53*, 679–689. [CrossRef]

37. Atkinson, P.J.; Powell, K.; Woodhead, C. Cortical structure of the pig mandible after the insertion of metallic implants into alveolar bone. *Arch. Oral Biol.* **1977**, *22*, 383–391. [CrossRef]

38. Powell, K.; Atkinson, P.J.; Woodhead, C. Cortical bone structure of the pig mandible. *Arch. Oral Biol.* **1973**, *18*, 171–180. [CrossRef]

39. Štembírek, J.; Kyllar, M.; Putnová, I.; Stehlík, L.; Buchtová, M. The pig as an experimental model for clinical craniofacial research. *Lab. Anim.* **2012**, *46*, 269–279. [CrossRef]

40. Gaffuri, S.; Audino, E.; Salvadori, M.; Garo, M.L.; Salgarello, S. Accuracy of a minimally invasive surgical guide in microsurgical endodontics: A human cadaver study. *G. Ital. Endod.* **2021**, *35*. [CrossRef]

41. Kim, S. *Color Atlas of Microsurgery in Endodontics*; Saunders: Hong Kong, China, 2001.

42. Younes, F.; Cosyn, J.; De Bruyckere, T.; Cleymaet, R.; Bouckaert, E.; Eghbali, A. A randomized controlled study on the accuracy of free-handed, pilot-drill guided and fully guided implant surgery in partially edentulous patients. *J. Clin. Periodontol.* **2018**, *45*, 721–732. [CrossRef] [PubMed]

43. Di Giacomo, G.A.; Cury, P.R.; de Araujo, N.S.; Sendyk, W.R.; Sendyk, C.L. Clinical application of stereolithographic surgical guides for implant placement: Preliminary results. *J. Periodontol.* **2005**, *76*, 503–507. [CrossRef] [PubMed]

44. Nickenig, H.J.; Wichmann, M.; Hamel, J.; Schlegel, K.A.; Eitner, S. Evaluation of the difference in accuracy between implant placement by virtual planning data and surgical guide templates versus the conventional free-hand method—A combined in vivo—In vitro technique using cone-beam CT (Part II). *J. Craniomaxillofac. Surg.* **2010**, *38*, 488–493. [CrossRef]

45. Arisan, V.; Karabuda, Z.C.; Ozdemir, T. Accuracy of two stereolithographic guide systems for computer-aided implant placement: A computed tomography-based clinical comparative study. *J. Periodontol.* **2010**, *81*, 43–51. [CrossRef] [PubMed]